The Art of Bone Scintigraphy—Technical Aspects

M.K. O'Connor, M. L. Brown, J.C. Hung, and R.J. Hayostek

Department of Radiology, Section of Nuclear Medicine Mayo Clinic, Rochester, Minnesota

J Nucl Med 1991; 32:2332-2341

Over the last 20 years, bone scintigraphy has grown to become one of the most commonly performed procedures in nuclear medicine, accounting for over half the studies performed in many nuclear medicine departments. Although a large number of review articles have discussed the current clinical status of radionuclide bone imaging (*1–6*), optimization of image quality has received little attention (*7*). Planar bone scintigraphy is simple and easy to perform. Nevertheless, there are a number of technical aspects that need to be considered in order to insure optimum image quality. The performance of tomographic bone studies represents a quantum leap in technical difficulty, and lack of attention to these technical aspects will result in the generation of suboptimal studies and artifacts in the image data (*8–9*).

The purpose of this article is to highlight the technical issues in radiopharmaceuticals and the importance of various imaging parameters on overall image quality for both planar and tomographic bone scintigraphy.

RADIOPHARMACEUTICALS

The first suitable radionuclides for bone scintigraphy, ^{85m}Sr, ^{87m}Sr, and ^{18}F, were introduced in the early 1960s (*10–12*). Of these ^{18}F, as sodium fluoride, was the most promising due to its rapid blood clearance and high affinity for bone (*11*). The major disadvantage of ^{18}F was its short half-life (110 min), which limited its availability to users in close proximity to a cyclotron. The introduction of ^{99m}Tc-phosphate complexes in the early 1970s brought the clinical use of ^{18}F in bone scintigraphy to a virtual halt. With the recent growth of positron emission tomography (PET), the production and availability of ^{18}F may no longer be a stumbling block to the clinical use of this radionuclide. Indeed, the use of ^{18}F as a bone tracer in PET may open up a new dimension in clinical bone scintigraphy (*13*).

Technetium-99m-polyphosphates were first successfully prepared and investigated by Subramanian and McAfee in 1971 (*14*). However, it was later found that the desirable bone-localizing properties of long-chain polyphosphates were primarily due to pyrophosphate either as an impurity or as a degradation product (*15*).

In the early 1970s, a different class of ^{99m}Tc-labeled agents, the diphosphonates, characterized by a P-C-P bond, were introduced for bone imaging (*16*). Unlike the early ^{99m}Tc-labeled poly- and pyrophosphates (P-O-P bond), the diphosphonates are more stable in vivo and have higher uptake in bone and more rapid blood clearance (*16*). It not clear how ^{99m}Tc-diphosphonate is incorporated into bone at the molecular level, however, it appears that regional blood flow, osteoblastic activity, and extraction efficiency are the major factors influencing uptake. In areas of increased osteogenic activity, active crystals of hydroxyapatite with large surface areas appear to be the most suitable sites for chemisorption of the diphosphonate ligands (*17*).

Approximately 50% of the dose of ^{99m}Tc-diphosphonate is distributed in the skeleton within 3 hr after intravenous administration, with the remainder excreted in the urine. In the normally hydrated patient, less than 5% of the dose remains in the blood 3 hr after injection. The critical organ site for dosimetry of ^{99m}Tc-diphosphonate is the bladder wall, due to its rapid urinary excretion.

Currently, ^{99m}Tc-methylene diphosphonate (MDP) and ^{99m}Tc-hydroxymethylene diphosphonate (HMDP or HDP) are the most commonly used radiopharmaceuticals for bone imaging. Comparison studies between MDP and HDP indicate that HDP has a 20% higher skeletal uptake than MDP (*18*). However, clinical comparisons between MDP and HDP show no significant difference in either lesion detectability or bone-to-soft tissue ratio (*19,20*).

All ^{99m}Tc bone complexes are fairly weak chelates and tend to degrade with time and produce free pertechnetate impurity. Consequently, bone kits with an antioxidant such as ascorbic acid or gentisic acid, will be most stable throughout their recommended time of use (*21,22*). Other factors such as the maximum ^{99m}Tc activity that can be added to the bone kit, the shelf life after labeling, and special storage conditions before/after labeling should also be considered when selecting a bone imaging product.

INSTRUMENTATION

While basic gamma camera technology has not changed over the last 15–20 yr, there have been incremental im-

Received Jan. 23, 1991; revision accepted Apr. 2, 1991.

For reprints contact: Dr. M. K. O'Connor, Section of Nuclear Medicine, Charlton Building, Mayo Clinic, Rochester, MN 55905.

provements in camera design and performance that have resulted in the availability today of dedicated whole-body imaging systems and dedicated multihead tomographic systems.

A number of manufacturers are now producing very large field of view dual-headed camera systems that permit the acquisition of simultaneous anterior and posterior whole-body images of a quality previously achievable only with conventional static images. Because of their large field of view (approximately 60 × 40 cm), these cameras eliminate the need for multiple passes along the body or the distortion introduced by single plane diverging collimators and can accommodate all but the largest patients.

Over the last few years, many of the exciting innovations in SPECT technology have been directed to improving the quality of SPECT neurologic studies. These improvements have concurrently improved the quality of other SPECT applications and have resulted in the appearance of several multi-detector dedicated SPECT units. Many of these units have a limited field of view in the axial direction, but offer the advantages of increased speed and throughput as well as improved resolution through better gantry design and collimation.

Many manufacturers now offer computer systems that are capable of acquiring planar, whole-body, and tomographic data. While the two former acquisition modes are generally of little importance in routine bone scintigraphy, the ability to easily acquire anterior and posterior whole-body images may lead to renewed interest in quantitation of tracer uptake (*23*). For SPECT, most computers now offer 32-bit architecture and some type of array processor to permit rapid processing of the tomographic data. The increased speed of these newer systems now offers the possibility to use other reconstruction techniques (e.g., Maximum Likelihood, ART) to further improve the reconstructed image quality without incurring a heavy time penalty.

One of the more interesting developments in bone imaging over the last one to two years has been the use of PET to produce ^{18}F whole-body bone scans (*13*). Current PET scanners are not ideally suited to this application, due to their limited field of view in the axial direction and the need for approximately 1 hr of scan time for a whole-body study (*24*). However, as Figure 1 illustrates, their high resolution coupled with the strong avidity of bone for the ^{18}F ion yield a significant improvement in image quality over that obtainable with conventional planar or SPECT technology.

ACQUISITION OF PLANAR and WHOLE-BODY IMAGES WITH ^{99m}Tc AGENTS

There are four primary acquisition parameters that can affect the quality of planar and whole-body scintigraphy. These are: (a) choice of collimator, (b) number of counts acquired, (c) distance of patient from the collimator, and (d) use of scatter reduction techniques. In general, the best

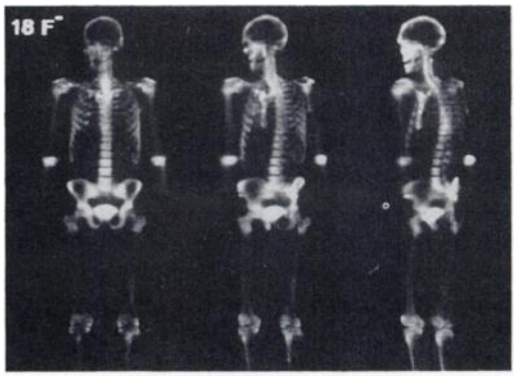

FIGURE 1. Whole-body PET bone scan with ^{18}F in a normal male subject. The images are two-dimensional projections of 3 of 32 different display angles. The complete 32-image set can be displayed on a computer monitor in a cine mode for a pseudo three-dimensional display (Courtesy of Doctors Hawkins and Hoh, UCLA Medical Center).

images will be obtained with an ultra high-resolution collimator, greater than 1M cts/image, no separation between patient and collimator, and the use of scatter reduction techniques, particularly in obese patients. In practice, use of the above parameters may not be feasible in the clinical environment. Below is a discussion of each of these parameters and an examination of their affect on image quality.

Collimation

Figure 2 compares three identical images of the pelvic region obtained with an ultra high-resolution, high-resolution, and all-purpose collimator. All three images contain 1M cts, with acquisition times of 14, 7, and 4 min, respectively. There is an incremental improvement in image quality between images acquired with the all-purpose, high-resolution, and ultra high-resolution collimators, however, the long imaging time required with the ultra high-resolution collimator generally precludes its use from routine clinical practice. Hence, for most planar and whole-body imaging, the high-resolution collimator appears to offer the best compromise between resolution and imaging time.

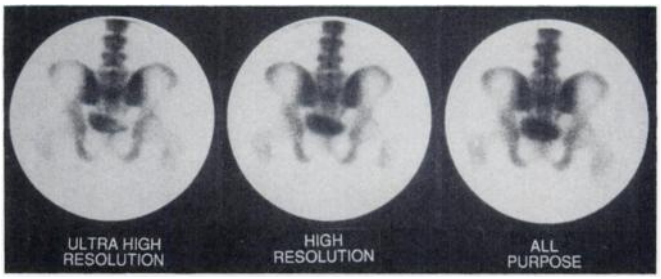

FIGURE 2. Images of the lumbar spine acquired using (A) ultra-high-resolution, (B) high-resolution, and (C) all-purpose collimator. All images were acquired for 1M cts. (LFOV 75 PM tube gamma camera, collimator resolution = 4.4, 6.4 and 8.2 mm at 10 cm in air for images (A), (B), and (C), respectively).

A high-resolution collimator may not be necessary for some imaging applications. In particular, images of the hands and feet or spot views of a hip may be better obtained with an all-purpose or pinhole collimator. Figure 3 compares hand and wrist views acquired using high-sensitivity, all-purpose, and high-resolution collimators. All views were acquired for 400K cts. There is a negligible difference in image quality between the three views due to the similarity in system resolution at the collimator surface (system resolution = 4.8, 4.4 and 4.2 mm for high-sensitivity, all-purpose, and high-resolution collimators, respectively, at surface). Hence, for imaging of the hands, wrists, or feet, an all-purpose or high-sensitivity collimator will provide similar resolution with a two- to three-fold increase in sensitivity.

High-resolution images of a small region can often be best obtained using a pinhole collimator. This collimator offers very good resolution and reasonable efficiency at imaging distances of less than 10 cm. Figure 4 illustrates this point by comparing two images of a hip obtained with pinhole and high-resolution collimators.

Image Counts

Many studies have shown that the ability to detect an abnormality within an image varies with the total number of counts acquired (*25*). For imaging of the axial skeleton, it is recommended that between 800 and 1500K cts be acquired per view for a 40-cm LFOV gamma camera, with 400–800K cts per view for extremity imaging (*1*). Figure 5 illustrates the affects of increasing image counts on image quality. At least 500 to 1000K cts are needed to detect subtle changes in tracer concentration and to adequately define anatomical location. For whole-body scans, this translates to approximately 2.5–3.5M cts per view.

Short imaging times will occasionally be required in patients who are uncooperative or are in pain and unable to tolerate the longer scan times. The modern dual-headed whole-body cameras greatly facilitate the imaging of such patients. Figure 6 presents anterior and posterior whole-body images with total acquisition times of 20 min, 6 min, and 70 sec. While subtle lesions may be missed on the 6-min scan, it provides sufficient information to permit, for example, the staging of known metastatic disease in a patient who is unable to remain still for a longer period of time.

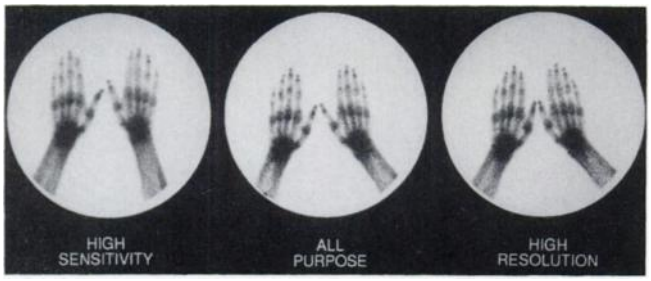

FIGURE 3. Hand views acquired for 400K cts/view on (A) a high-sensitivity, (B) all-purpose, and (C) high-resolution collimator. Imaging times were 7.5, 14.5, and 23.5 min, respectively.

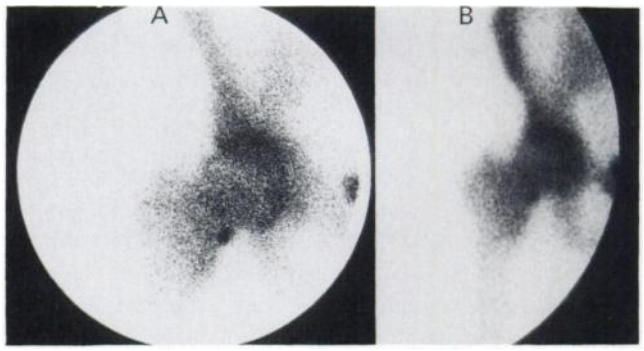

FIGURE 4. Images of a hip obtained with (A) pinhole collimator with a 6-mm aperture and (B) high-resolution collimator (× 2.0 magnification). Imaging times were 12 and 7 min, respectively.

Distance

Figure 7 illustrates the effects of increasing patient-to-collimator distance on image resolution. While collimator sensitivity remains unchanged over the 0–30 cm range, the overall system resolution in air typically degrades from 4–5 mm at 0 cm to 17–18 mm at 30 cm for a high-resolution collimator. An even larger degradation in resolution with distance occurs with all-purpose and high-sensitivity collimators. Failure to minimize the patient-to-collimator distance is probably one of the most common causes of suboptimal image quality in nuclear medicine.

Scatter Reduction

The final acquisition parameter that can improve image quality is the use of scatter reduction techniques such as an asymmetrical energy window setting (*26,27*) or preferential weighting of the energy spectrum (*28,29*). While these techniques are most beneficial in the imaging of radionuclides such as ^{67}Ga, ^{111}In, and ^{201}T1, they can yield a noticeable improvement in image quality for bone scintigraphy, particularly in the more obese patient. Figure 8 presents three images of the lumbar spine obtained using various scatter reduction techniques in a moderately obese patient. The improvement in image contrast is most noticeable in the disk spaces and in the definition of the ribs.

While each of the above parameters, taken alone, may only have a marginal effect, their combined effect can have an impact on image quality that is clinically significant. To illustrate this point, Figure 9 presents two images of the lumbar spine obtained with different sets of acquisition parameters. Like many other aspects of life, high quality bone scintigraphy requires attention to detail and a commitment to excellence.

DISPLAY AND HARD COPY

Depending on the gamma camera/computer system, hard copy of planar bone images may be in analog or

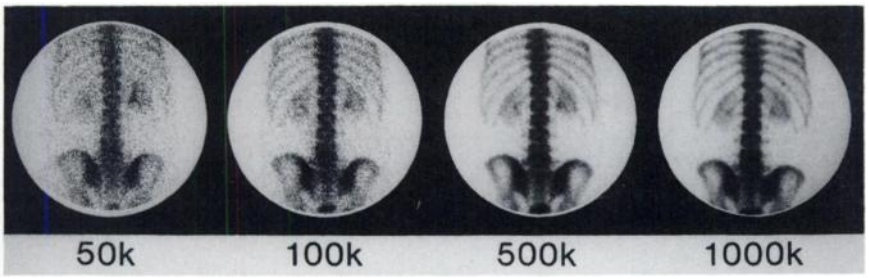

FIGURE 5. Images of the lumbar spine acquired using a high-resolution collimator. Total counts per view are indicated in K cts. (50 cm FOV, 91 PM tube gamma camera).

digital (video) format. There are advantages and disadvantages to both types of hard copy techniques. With an analog formatter, incorrect intensity setting requires a repeat acquisition. However, once the correct setting is established for a particular type of study, the analog formatter provides reliable image quality. The optical density (i.e., blackness of the film) is limited only by the film characteristics and can have a maximum value of greater than 3.5. The factors which require monitoring on an analog formatter are image size (i.e., images should be circular and not overlap each other), consistent optical density for like images over the entire film, and dot size. The first two factors can be evaluated with a series of flood images (*30*). The dot size used to create each image can be evaluated by increasing the dot intensity to maximum and acquiring background images for 10–30 sec. The influence of dot size will be dependent on image hard copy format and on the number of counts in an image. For a high count image, increasing dot size will act as a smoothing filter and will decrease image intensity. For low count images (e.g., flow study), the decrease in image intensity with increasing dot size may be severe enough to prevent adequate visualization of tracer flow.

Video formatters are generally more subject to drift than analog formatters and are highly dependent on the contrast and brightness settings. Depending on the design of the formatter, they are also susceptible to dust buildup on the monitor face, leading to a gradual reduction in image brightness over time. Correct setup can be achieved through the use of a test pattern such as the SMPTE (*31*). Video formatters are normally set up to achieve a more limited optical density range on film than analog formatters, typically from 0 to 2.2 (*32*). Hence, a video formatter can never truly mimic the performance of an analog formatter. While this difference is not important in hard copying a normal bone scan, it poses difficulties if extremely hot regions are present in a scan (e.g., hot bladder, Paget's disease). These hot regions can be accommodated in an analog formatter, but lead to suppression of low count image data in a video formatter. Furthermore, due to the inherent difference in how an image is formed in analog and video formatters, the relationship between optical density and image counts is not the same. A partial solution to this problem is to use a translation table or grey scale map on the computer that will permit the video formatter to mimic an analog formatter over the optical

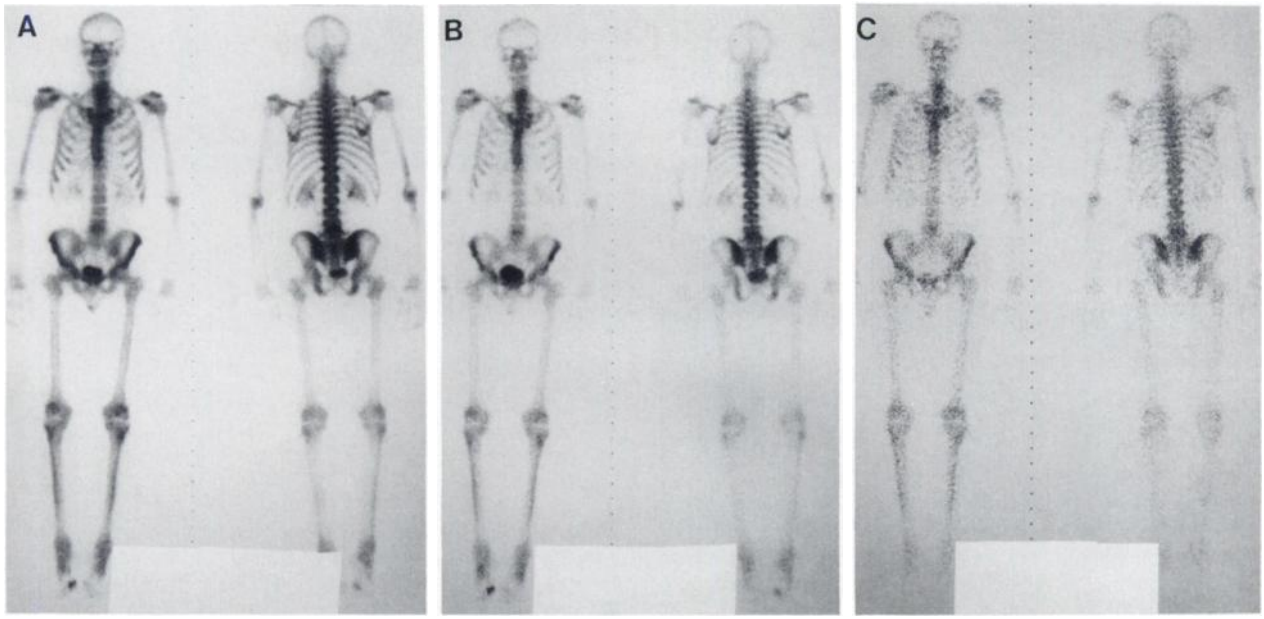

FIGURE 6. Anterior and posterior whole-body images of the same patient acquired for (A) 20 min (B) 6 min, and (C) 70 sec (two 63 × 40 cm FOV detectors with high-resolution collimators).

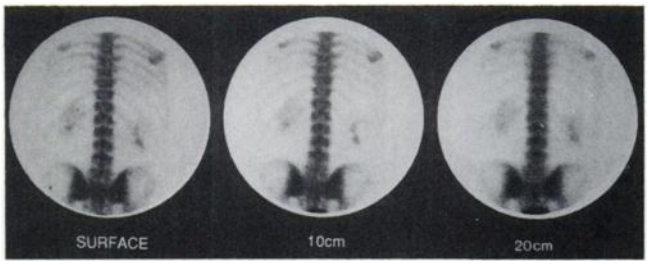

FIGURE 7. Images of the lumbar spine acquired using a high-resolution collimator with 1M cts/view. Distance from collimator face to patient varied from 0–20 cm (50 cm FOV, 91 PM tube gamma camera).

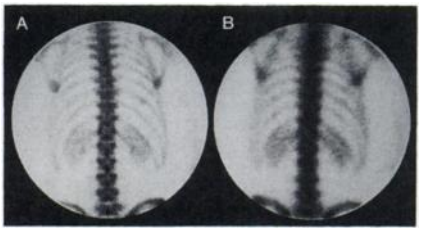

FIGURE 9. Posterior images of the lumbar spine in the same patient acquired with (A) high-resolution collimator, 1M cts, no patient-to-collimator separation and scatter rejection, and (B) all-purpose collimator, 400K cts, 10 cm patient-to-collimator separation and no scatter rejection. Time/image was 9 and 2 min for (A) and (B), respectively.

density range 0–2.2. Figure 10 illustrates the affects of different grey scale maps on the hard copy appearance of bone images. A full description of how such grey scale maps can be created is beyond the scope of this article, but a number of useful references are available on this subject (*33,34*).

The quality of the image hard copy from the video formatter will also be affected by the size of the acquisition matrix. For bone imaging, it has been shown that a matrix size of 256 × 256 is desirable for large and jumbo field of view gamma cameras (*35*). For whole-body images, a 1024 × 256 matrix size will provide comparable image quality.

PLANAR AND WHOLE-BODY IMAGING—SUMMARY

To summarize the above, we would recommend that for routine bone scintigraphy, a high-resolution collimator be used, patient-to-collimator distance be kept as close as reasonably achievable (the ACARA principle!), hard copy devices be checked to assure optimum image reproduction and, where possible, that scatter reduction techniques be employed. The number of counts per image will depend on the gamma camera field of view and the region being imaged, but as a general rule, for a 40-cm field of view gamma camera, 1M cts should be acquired over the thoracic spine with other images being acquired for a similar time per image.

We have not made any recommendations as to the most suitable patient position, i.e., upright versus supine versus sitting, etc. For spot views, this should be dictated by the ACARA principle, while recognizing that the imaging position must be such that it minimizes the likelihood of patient motion and can be tolerated by the patient without undue discomfort. With this in mind, there are a number of studies that discuss the benefit of various patient maneuvers to enhance the visualization of particular parts of the skeleton such as the hips, shoulders, and thoracic and lumbar vertabrae (*36–39*).

SPECT: ACQUISITION PARAMETERS

The quality of a bone SPECT study can only be as good as the quality of the planar images used to create that

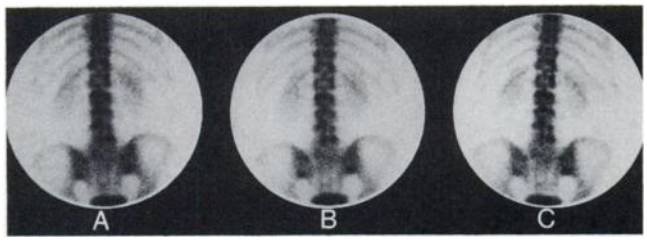

FIGURE 8. Images of the lumbar spine acquired using a high-resolution collimator. All images were acquired for the same time, with 1M cts in the conventional image (A). Images (B) and (C) were obtained using a 5.6% asymmetrical energy window and a weighted energy acquisition method, respectively.

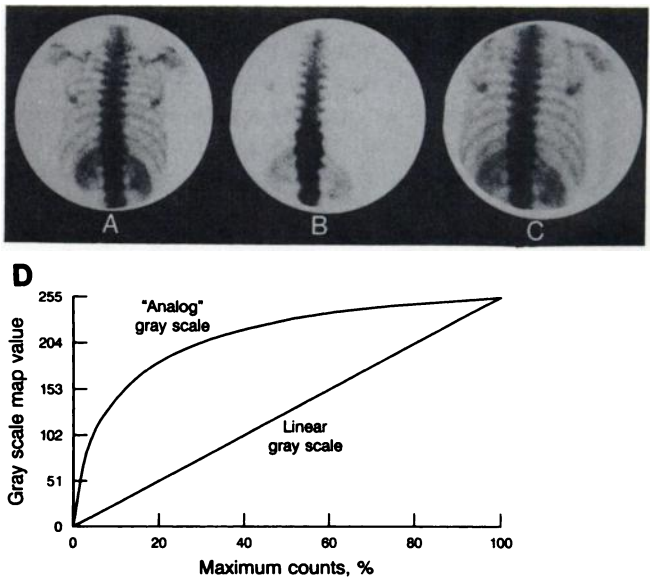

FIGURE 10. Posterior images of the lumbar spine in a patient with Paget's disease shown in analog format (A) and in digital format (256 × 256 matrix) obtained using a linear grey scale ramp (B) and a modified grey scale designed to mimic an analog formatter (C). The shapes of the linear and modified grey scale ramps are shown in (D).

study. Hence, all of the factors discussed above for planar imaging pertain also for SPECT imaging. There are, however, a number of additional factors that need to be considered for SPECT.

Collimation

With the limited time/view (approximately 20–40 sec) in SPECT, there is a trade-off between resolution and adequate counting statistics. Several studies have shown that for bone SPECT, high-resolution/low-count studies are superior to low-resolution/high-count studies (*40,41*).

Matrix Size

To take advantage of a high-resolution collimator, a 128 × 128 acquisition matrix should be used. For brain SPECT, it is possible to use a 64 × 64 matrix with a 1.5–2.0 zoom instead. If a zoom mode is used, care should be taken to ensure that the entire head is within the field of view of the gamma camera on all views. Figures 11A, C, D illustrate the affects of various collimators and matrix sizes on image quality. There is a clear improvement in image quality with increased matrix size and with higher resolution collimation.

Three Hundred- Versus 180-Degree Acquisition

Although 360-degree orbits are the norm for bone SPECT, there are occasions when a 180-degree acquisition may be preferable. Figures 11A–B compare two coronal views of the same subject acquired with 360- and 180-degree rotations. With the 180-degree rotation, there is increased contrast and better lesion detectability in the lumbar spine but with increased distortion as one moves away from the center of the image. Hence, 180-degree acquisition may be preferable in cases where only the spine is being evaluated and where a short distance between collimator and patient cannot be maintained with a 360-degree orbit. If a 180-degree orbit is used, the patient should be imaged prone to eliminate table attenuation and to minimize collimator to patient distance.

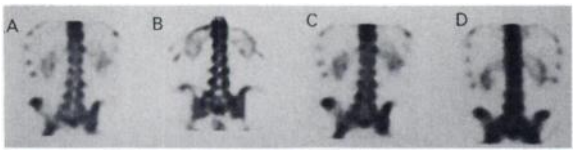

FIGURE 11. Coronal slices through the lumbar spine from four studies of the same subject. All studies were acquired for 40 sec/view with 64 views and reconstructed with a Butterworth filter, order 10, cutoff at 0.45 Nyquist. Studies were done with (A) high-resolution collimator, 128 matrix, 360-degree orbit, (B) high-resolution collimator, 128 matrix, 180-degree orbit, (C) high-resolution collimator, 64 matrix, 360-degree orbit and (D) all-purpose collimator, 64 matrix, 360-degree orbit.

Angular Sampling Requirements

The angular sampling requirements for SPECT are determined by the relationship between organ size and system resolution (*42,43*). For a 128 matrix, approximately 40, 70, and 110 views are required for complete angular sampling of the spine, head, and pelvic regions, respectively. In practice, 60–70 views are adequate for most clinical studies (*44*). Increasing the number of views to 120–130 may lead to better definition of structures such as the ribs, but there is the penalty of increased disk storage requirements and longer reconstruction times.

Elliptical/Circular Orbit

Elliptical orbits generally involve movement of the gamma camera gantry or patient table during acquisition in order to achieve closer collimator to patient distance throughout the orbit. Image resolution achieved with an elliptical orbit will be patient-dependent but will always be equal to or better than that achieved with a conventional circular orbit (*45,46*). Figure 12 illustrates the improvement in resolution obtained with elliptical versus circular orbit.

SPECT PROCESSING PARAMETERS

Prefiltering Versus Filtering During Reconstruction

Prefiltering involves applying the selected smoothing filter (e.g., Hann, Butterworth) to the planar data prior to backprojection. Since it smoothes the data along the axial direction, it effectively smoothes between transaxial slices and improves the quality of transaxial, coronal, and sagittal views. Prefiltering can also enhance image contrast and reduce image noise (*47*). Figure 13 presents two sagittal views of the same study reconstructed with identical filters. It can be seen that prefiltering eliminates discontinuities between rows in the image and provides a more acceptable image quality. Not all manufacturers provide the capability of prefiltering in their tomographic

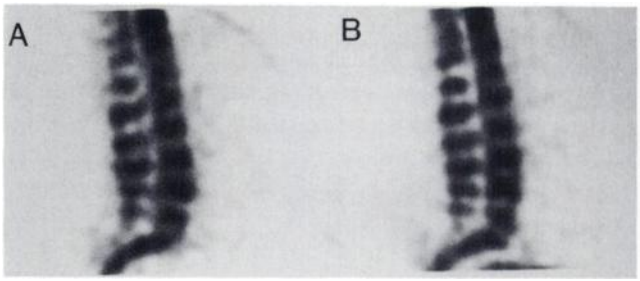

FIGURE 12. Sagittal slices through the spine from two studies of the same subject, each acquired over 360 degrees with 40 sec/view, 64 views, 128 matrix, high-resolution collimator and reconstructed with a Butterworth filter, order 10, cutoff at 0.45 Nyquist frequency. Studies were done using (A) circular orbit and (B) elliptical orbit.

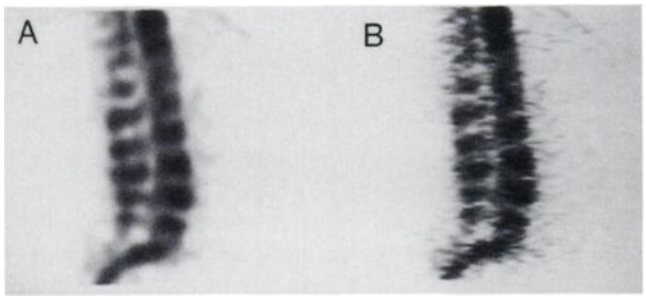

FIGURE 13. Sagittal views of a lumbar spine reconstructed with (A) pre-filtering and (B) filtering during backprojection (128 matrix, 64 views, Butterworth filter, order 10, cutoff at 0.45 Nyquist frequency).

software, and in such cases use of a temporal smoothing filter between transaxial slices will yield similar results.

Reconstruction Filters

The selection of the optimum filter is partly a matter of personal preference and partly dictated by the noise level in the images. A gamma camera with a high-resolution collimator can (potentially) resolve objects down to 6–7 mm in size. This corresponds to a spatial frequency of 0.7–0.8 cycles/cm, or 0.5 times Nyquist for a 128 × 128 matrix. Higher spatial frequencies can be eliminated without compromising image quality. This sets a good starting point for cutoff frequency. It may need to be reduced, depending on image noise, but should be set as high as possible, consistent with acceptable image quality, to preserve as much information as possible. Bone images contain high frequency information, hence, filters such as the Butterworth, that can be tailored to roll-off sharply, are better at preserving the information content of the images than a simple Hann filter.

SPECT BONE—SUMMARY

In summary, like planar imaging, optimum SPECT imaging generally requires the use of a high-resolution collimator and a 128 × 128 acquisition matrix, despite the limited counting statistics. If possible, an elliptical orbit should be used to minimize patient to collimator distance. Approximately 60–64 views should be acquired at 30–40 sec per view. Reconstruction should employ a prefilter (recommend using a Butterworth, order 8–12, cutoff at 0.4–0.5 Nyquist) and backprojection with a simple ramp filter. Attenuation correction is not normally beneficial in SPECT bone studies. Some computer systems offer additional software that can improve the quality of image reconstruction or enhance the display of the reconstructed data. Examples of such software include the use of distance-weighted backprojection to improve image contrast and resolution (*48,49*), and the use of volume rendering to better define the location of a lesion (*50*).

QUALITY CONTROL REQUIREMENTS—PLANAR AND SPECT

Planar and Whole-Body Gamma Cameras

Conventional uniformity and resolution images should be obtained on a daily and weekly basis, respectively. There are many helpful documents detailing the performance of such uniformity and resolution measurements (*51–53*). Additionally, the dot size on the analog formatter should be checked on a monthly basis. For video formatters, a suitable test pattern should be hard copied and checked on a weekly basis to verify that there is an appropriate optical density range on film and to ensure stability of the contrast and brightness settings (32). For whole-body imaging systems, an additional check of the uniformity of gantry speed over the length of the table should be made. This can be accomplished by placing a sheet source on top of one detector and performing a whole-body acquisition. The resulting whole-body flood image can be checked for fluctuations in uniformity along the length of the image (*54*).

SPECT

It is beyond the scope of this article to engage in a full discussion of the quality control requirements for SPECT (*8,9,55,56*), hence, we will confine this discussion to a brief review of the two most critical aspects of SPECT quality control: adequate image uniformity and correction for variations in center of rotation.

Although few studies have critically examined the uniformity requirements for SPECT (*57,58*), a 30M count extrinsic flood is generally considered to provide adequate uniformity correction for current clinical studies on a standard LFOV camera (*8,9*). Changing the acquisition matrix size from 64 × 64 to 128 × 128 does not appear to significantly change these requirements (*59*).

The purpose of uniformity correction in SPECT is to minimize nonuniformities in detector response. Hence, it is essential that the collimator be included in this process. By the very nature of the backprojection process, any nonuniformities in gamma camera response will be manifest as ring artifacts in the reconstructed transaxial images. The magnitude of the ring artifact will depend on the relative change in image uniformity from one pixel to the next and on the distance of this nonuniformity from the center of rotation. For this reason, a gradual change in image uniformity over the entire field of view is less critical than that same change occurring over a small region of the field of view.

For SPECT, we would recommend that image uniformity be measured using standard NEMA techniques (*51*). Briefly, the NEMA technique requires that the flood images be analyzed in a 64 × 64 matrix, undergo a nine-point smooth, and the maximum variation in pixel counts over the useful field of view (integral uniformity) and over a floating five-pixel wide band within the useful field of

view (differential uniformity) be determined. Because it measures local variation in uniformity, differential uniformity is the best indicator of the adequacy of a uniformity correction map for SPECT.

Quality control in SPECT requires that not only is a uniformity correction map required, but that the validity of this map is checked on a daily basis. To do this, one should in theory, acquire another flood image of adequate statistical accuracy, apply the correction map to it, and measure its uniformity as described above. Since this is not practical on a daily basis, a common alternative is to acquire a low count flood image (approximately 2–3M counts), apply uniformity correction to it, and visually inspect it for residual nonuniformities. A more precise and quantitative alternative is to acquire a 7–10M counts flood, apply uniformity correction and smoothing, compress the corrected image to a 32 × 32 matrix to yield adequate counting statistics, and measure uniformity. In our experience, a SPECT system in good working order will have values of differential uniformity in the range 1.5%–3.0% with integral uniformity being slightly larger (2%–4%).

The center or rotation of a SPECT system should be determined solely by the mechanical setup of the gantry and the relationship between the image and the computer matrix. In practice, the collimator can also alter both the global center of rotation and can cause local variations in center of rotation over the collimator face. Current indications are that approximately 25%–30% of all collimators are unsuitable for SPECT primarily because of hole angulation errors (*60,61*). There are a number of simple techniques that will allow quantitation of hole angulation errors in collimators (*60,62*). A general recommendation is that the center of rotation should vary by less than ±1.5 mm (at a radius of 20 cm) over the useful field of view (*61*). With good mechanical stability of the gantry, there should be less than 0.5 pixel (128 × 128 matrix) variation in center of rotation over 360 degrees.

SPECT ARTIFACTS

While most of us are familiar with the classic examples of ring artifacts, their appearance in clinical practice often can be extremely deceiving. Figure 14 presents an example of a ring artifact in a bone SPECT study. This type of artifact can be caused by something as simple as a dent in the collimator and can easily be interpreted as pathology. It demonstrates the need for adequate quality control to ensure satisfactory performance of a SPECT system.

Errors in center of rotation have a less dramatic impact on image quality and deviations of between 2–4 mm from the true center of rotation will cause blurring of the reconstructed images. Larger errors in center of rotation can cause significant distortion of the data. Figure 15 illustrates the effects of 3.2 mm (1 pixel) and 9.6 mm (3 pixel) deviations in the center of rotation on transaxial image quality.

TYPES OF BONE EXAMINATIONS

In general, bone scintigraphy can be considered as a survey technique to evaluate patients with malignancies, diffuse musculoskeletal symptoms, abnormal laboratory results, and hereditary or metabolic disorders. The other major application of bone scintigraphy is in the evaluation of patients with suspected localized disease such as focal pain or trauma or the assessment of abnormalities detected on other imaging modalities.

For bone survey techniques, high quality, high count rate studies can be obtained as either multiple spot views or as anterior and posterior whole-body images. In all cases, the initial images should be reviewed and appropriate additional views such as obliques, laterals, postvoiding pelvic views, arm-up scapular views, etc., should be obtained to completely define the location and extent of any questionable abnormality.

Three-phase bone scintigraphy is helpful in areas of suspected trauma and musculoskeletal sepsis. The flow phase and early soft-tissue phases will be positive for very active processes and may help in determining whether the abnormalities are recent. When three-phase scintigraphy is used to evaluate suspected abnormalities in the hands and wrists, care must be taken to avoid the reflex vasodilatation, the so-called "tourniquet effect." This can be accomplished by either not using a tourniquet when placing the needle into the vein or by releasing the tourniquet and waiting approximately 5 min before injecting the radiopharmaceutical (*63*).

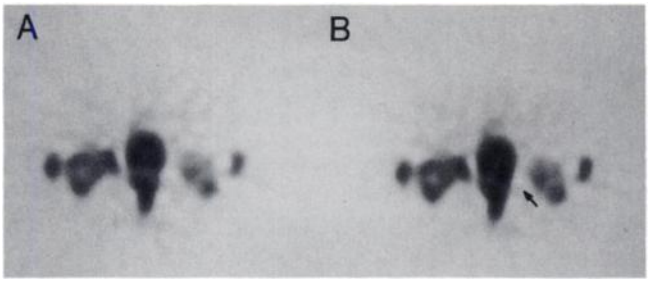

FIGURE 14. Transaxial slices through the lumbar spine generated (A) with and (B) without uniformity correction. Arrow indicates the location of a ring artifact in the uncorrected image.

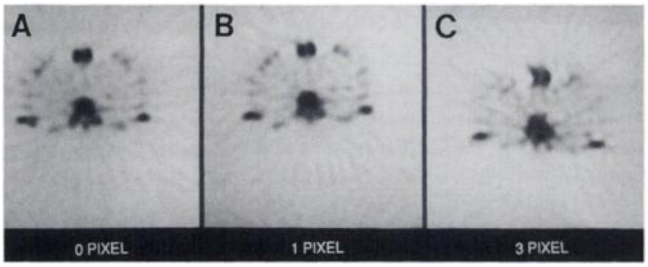

FIGURE 15. Transaxial slices through the thoracic spine generated using (A) true center of rotation, (B) one pixel offset, and (C) three pixel offset in center of rotation (128 × 128 matrix).

When studying areas such as the hands and feet, the patient should be positioned so that the appropriate portion of the extremity is in direct contact with the collimator. For views of the feet, shoes should be removed prior to imaging. As noted above, oblique views, lateral views, etc., should be obtained liberally to fully localize the areas of abnormality.

SPECT imaging in bone scintigraphy has been shown to be very useful in evaluating the skull (*64,65*), spine (*66,67*), hips (*68,69*), and knees (*70,71*). The two areas that have received the most attention are the head and spine. The indications for SPECT in the head include the evaluation of TMJ abnormalities and the assessment of the extent of malignant external otitis, sinus infections, etc. The major use of SPECT in the spine includes the detection or assessment of spondylosis and the detection of pseudarthroses in patients who have undergone spinal fusion surgery.

CONCLUSIONS

In this technical review, we have attempted to study the principal factors governing image quality in bone scintigraphy. Many of the principles we have presented above are common knowledge. Nevertheless, we believe that the consequences of not applying these principles, in terms of image quality, is often not fully appreciated. We hope that the above will remind all concerned to review their current practices for bone scintigraphy and enhance the quality of their clinical studies.

REFERENCES

1. Holder LE. Clinical radionuclide bone imaging. *Radiology* 1990;176:607–614.
2. Silberstein EB, Brown ML, Rosenthall L, Wahner HW. Skeletal nuclear medicine. In: Siegel BA, Kirchner PT, eds. *Nuclear medicine: self-study program I.* New York: Society of Nuclear Medicine; 1988:93–131.
3. Merrick MR. Bone scintigraphy: an update. *Clin Radiol* 1989;40:231–232.
4. Fogelman I, ed. *Bone scanning in clinical practice.* London: Springer-Verlag; 1987.
5. Mettler FA Jr, ed. *Radionuclide bone imaging and densitometry: contemporary issues in nuclear medicine, volume 4.* New York: Churchill Livingstone; 1988.
6. Freeman LM, Blaufox MD, eds. Nuclear orthopedics. *Semin Nucl Med* 1988;18:77–158.
7. Merrick MV. The normal bone scan. In: Fogelman I, ed. *Bone scanning in clinical practice.* London: Springer-Verlag; 1987:19–29.
8. Harkness BA, Rogers WL, Clinthorne NH, Keyes JW. SPECT: quality control procedures and artifact identification. *J Nucl Med Technol* 1983;11:55–60.
9. Todd-Pokropek A. Quality control and assurance of single photon emission computerized tomographic (SPECT) systems. *Ann Radiol* 1983;26:23–30.
10. Charkes ND, Sklaroff DM. Early diagnosis of metastatic bone cancer by photoscanning with strontium-85. *J Nucl Med* 1964;5:168–179.
11. Blau M, Nagler W, Bender MA. Fluorine-18. A new isotope for bone scanning. *J Nucl Med* 1962;3:332–334.
12. Charkes ND. Some differences between bone scans made with Sr-87m and Sr-85. *J Nucl Med* 1969;10:491–494.
13. Hoh C, Hawkins RA, Dahlbom M, et al. Total-body and cross-sectional imaging of the skeletal system with F-18 and PET [Abstract]. *J Nucl Med* 1990;31:780.
14. Subramanian G, McAfee JG. A new complex of Tc-99m for skeletal imaging. *Radiology* 1971;99:192–196.
15. Davis MA, Jones AG. Comparison of 99m-Tc labeled phosphate and phosponate agents for skeletal imaging. *Semin Nucl Med* 1976;6:19–31.
16. Subramanian G, McAfee JG, Blair RJ, et al. Technetium-99m-methylene diphosponate—a superior agent for skeletal imaging. Comparison with other technetium complexes. *J Nucl Med* 1975;16:744–755.
17. Francis MD, Tofe AJ, Benedic JJ, et al. Imaging the skeletal system. In: Sorenson JA, ed. *Radiopharmaceuticals II.* New York: Society of Nuclear Medicine; 1974:603–614.
18. Fogelman I, Pearson DW, Bessent RG, et al. A comparison of skeletal uptakes of three diphosphonates by whole-body retention. *J Nucl Med* 1981;22:880–883.
19. Rosenthal L, Arzoumanian A, Damtew B, et al. A crossover study comparing Tc-99m-labeled HMDP and MDP in patients. *Clin Nucl Med* 1981;6:353–355.
20. Delaloye B, Delaloye-Bischof A, Dudczak R, et al. Clinical comparison of ^{99m}Tc-HMDP and ^{99m}Tc-MDP. A multicenter study. *Eur J Nucl Med* 1985;11:182–185.
21. Tofe AJ, Francis MD. In vitro stabilization of a low-tin bone imaging agent (^{99m}Tc-HEDP) by ascorbic acid. *J Nucl Med* 1976;17:820–825.
22. Tofe AJ, Bevan JA, Fawzi MB, et al. Gentisic acid: a new stabilizer for low tin skeletal imaging agents. *J Nucl Med* 1980;21:366–370.
23. Smith ML. Quantitative ^{99m}Tc-diphosphonate uptake measurements. In: Fogelman I, ed. *Bone scanning in clinical practice.* Berlin: Springer-Verlag; 1987:237–248.
24. Dahlbom M, Schiepers C, Hoffman EJ, et al. Evaluation of PET for whole-body imaging [Abstract]. *J Nucl Med* 1990;31:749.
25. Biberman LM, ed. *Perception of displayed information.* New York: Plenum; 1973.
26. Collier BD, Palmer DW, Knobel J, et al. Gamma camera energy windows for Tc-99m bone scintigraphy: effect of asymmetry on contrast resolution. *Radiology* 1984;151:495–497.
27. LaFontaine R, Stein MA, Graham LS, Winter J. Cold lesions: enhanced contrast using asymmetric photopeak windows. *Radiology* 1986;160:255–260.
28. Halama JR, Henkin RE, Friend LE. Gamma camera radionuclide images: improved contrast with energy-weighted acquisition. *Radiology* 1988;169:533–538.
29. Wirth V. Effective energy resolution and scatter rejection in nuclear medicine. *Phys Med Biol* 1989;34:85–90.
30. Fajman WA, Sarper R. Multiimage formatting: effect on scintillation image quality. *AJR* 1982;139:751–754.
31. Society of Motion Picture and Television Engineers. Specifications for medical diagnostic imaging test pattern for television monitors and hard-copy recording devices. *SMPTE J* 1986;95:693–695.
32. Gray JE, Lisk KG, Haddick DH, et al. Test pattern for video displays and hard-copy cameras. *Radiology* 1985;154:519–527.
33. Rogers WL, Keyes JW Jr. Techniques for precise recording of grey scale images from computerized scintigraphic images. *J Nucl Med* 1981;22:283–286.
34. Muller C, Wasserman HJ, Erlank P, Klopper JF, Morkel HR, Ellmann A. Optimisation of density and contrast yielded by multiformat photographic imagers used for scintigraphy. *Phys Med Biol* 1989;34:473–481.
35. Sharp PF, Chesser RB, Mallard JR. The influence of picture element size on the quality of clinical radionuclide images. *Phys Med Biol* 1982;27:913–926.
36. Schutte HE. Some special views in bone scanning. *Clin Nucl Med* 1980;5:172–173.
37. Yu J, Ford P, Chen DCP, Arnstein N, Siegel ME. Improvement of the posterior spine in resolution of bone scintigraphy with sitting position [Abstract]. *J Nucl Med Technol* 1988;16:ab4.
38. Ford PV, Hung GL, Chen DCP, Arnstein NB, Siegel ME. Upright spine scintigraphy: a means of improving anatomic definition [Abstract]. *J Nucl Med* 1987;28:664.
39. Shryock M, Greenwell M, Henry J, Ryo UY. Advantages and pitfalls of sitting view pelvic bone scan [Abstract]. *J Nucl Med Technol* 1988;16:Ab3.
40. Muehllehner G. Effect of resolution improvement on required count density in ECT imaging: a computer simulation. *Phys Med Biol* 1985;30:163–173.
41. Mueller SP, Polak JF, Kijewski MF, Holman BL. Collimator selection for SPECT brain imaging: the advantage of high resolution. *J Nucl Med* 1986;27:1729–1738.
42. Phelps ME. Emission computed tomography. *Semin Nucl Med* 1977;7:337–365.
43. Oppenheim BE, Appledorn CR. Single photon emission computed tomography. In: Gelfand MJ, Thomas SR, eds. *Effective use of computers in nuclear medicine.* New York: McGraw Hill; 1988:31–74.
44. Schiepers CWJ, Lee KH, Siegel ME. The effects of angular sampling

frequency in SPECT on image quality: phantom and clinical studies [Abstract]. *Eur J Nucl Med* 1989;15:559.
45. Gottschalk SC, Salem D, Lim CB, Wake RH. SPECT resolution and uniformity improvements by noncircular orbit. *J Nucl Med* 1983;24:822–828.
46. Esser P, Jakimcius A, Foley L. The peanut orbit: a modified elliptical orbit for single-photon emission computed tomography imaging. *Med Phys* 1989;16:114–118.
47. Madsen MT, Park CH. Enhancement of SPECT images by Fourier filtering the projection image set. *J Nucl Med* 1985;26:395–402.
48. Nowak DJ, Eisner RL. Fajman WA. Distance-weighted backprojection: a SPECT reconstruction technique. *Radiology* 1986;159:531–536.
49. Hellman RS, Nowak DJ, Collier BD, Isitman A, Eisner R. Evaluation of distance weighted SPECT reconstruction for skeletal scintigraphy. *Radiology* 1986;159:473–475.
50. Wallis JW, Miller TR. Volume rendering in three-dimensional display of SPECT images. *J Nucl Med* 1990;31:1421–1430.
51. Raff U, Spitzer VM, Hendee WR. Practicality of NEMA performance specification measurements for user-based acceptance testing and routine quality assurance. *J Nucl Med* 1984;25:679–687.
52. Patton DD. Gamma camera quality control. *Clin Nucl Med* 1979;4:482–485.
53. Graham LS. Quality assurance of anger cameras. In: Rao DV, Chandra R, Graham MC, eds. *Physics of nuclear medicine: recent advances.* New York: American Institute of Physics; 1984:68–82.
54. Jackson PC. *Radionuclide imaging in medicine.* New York: Alan R. Liss; 1986:177–204.
55. English RJ, Zimmerman RE. Performance and acceptance testing of scintillation cameras for SPECT. *J Nucl Med Technol* 1988;16:132–138.
56. Murphy PH. Acceptance testing and quality control of gamma cameras, including SPECT. *J Nucl Med* 1987;28:1221–1227.
57. Gullberg GT. An analytical approach to quantify uniformity artifacts for circular and noncircular motion in single photon emission computed tomography imaging. *Med Phys* 1987;14:105–114.
58. Rogers WL, Clinthorne NH, Harkness BA, Koral KF, Keyes JW. Field-flood requirements for emission computed tomography with an anger camera. *J Nucl Med* 1982;23:162–168.
59. O'Connor MK, Vermeersch C. A critical examination of the uniformity requirements for single photon emission computed tomography. *Med Phys* 1991;18:190–197.
60. Busemann-Sokole E. Measurement of collimator hole angulation and camera head tilt for slant-hole and parallel-hole collimators used in SPECT. *J Nucl Med* 1987;28:1592–1598.
61. O'Connor MK, Oswald WM. Influence of collimators on SPECT center of rotation measurements. *J Nucl Med* 1989;30:265–266.
62. Cerqueira MD, Matsuoka D, Ritchie JL, Harp GD. The influence of collimators on SPECT center of rotation measurements: artifact generation and acceptance testing. *J Nucl Med* 1988;29:1393–1397.
63. Lecklitner ML, Douglas KP, Skeletal scintigraphy of the hands and wrists: trauma, tumors, infections and other inflammation. In: Freeman LM, Weissmann HS, eds. *Nuclear medicine annual 1986.* New York: Raven Press, 1986:247–283.
64. Israel O, Jerushalmi J, Frenkel A, et al. Normal and abnormal single photon emission computed tomography of the skull: comparison with planar scintigraphy. *J Nucl Med* 1988;29:1341–1346.
65. Collier BD, Carrera GF, Messer EJ, et al. Internal derangements of the temporomandibular joint: detection by single photon emission computed tomography. *Radiology* 1983;149:557–561.
66. Jacobsson H, Larsson SA, Vestersklod L, et al. The application of single photon emission computed tomography to the diagnosis of ankylosing spondylitis of the spine *Br J Radiol* 1984;57:133–140.
67. Lusins JO, Danielski EF, Goldsmith SJ. Bone SPECT in patients with persistant back pain after lumbar spine surgery. *J Nucl Med* 1989;30:490–496.
68. Stromqvist B, Brismar J, Hansson LI. Emission tomography in femoral neck fracture for evaluation of avascular necrosis. *Acta Orthop Scand* 1983;54:872–877.
69. Collier BD, Carrera GF, Johnson RP, et al. Detection of femoral head avascular necrosis in adults by SPECT. *J Nucl Med* 1985;26:979–987.
70. Gupta SM, Foster CR, Kayani N. Usefulness of SPECT in the early detection of avascular necrosis of the knees. *Clin Nucl Med* 1987;12:99–102.
71. Collier BD, Johnson RP, Carrera GF, et al. Chronic knee pain assessed by SPECT: comparison with other modalities. *Radiology* 1985;157:795–802.